

NICMOS Pointed Thermal Background: Results from On-Orbit data.

Doris Daou and Chris Skinner
October 14, 1997

ABSTRACT

This ISR presents the results of the analysis of NICMOS pointed thermal background data taken as part of the Servicing Mission Orbital Verification (SMOV). Observations in NICMOS Camera 3 are taken at different pointings and analysis of the data shows the HST thermal emission to be fairly stable. Furthermore, data obtained with multiple filters shows no significant differences with the background calculated with the NICMOS Exposure Time Calculator.

1. Introduction

During observations with NICMOS, thermal emission from the HST OTA reaches the instrument's focal plane. In order to measure and characterize the HST thermal background effects on NICMOS, a test was performed as a part of the Servicing Mission Orbital Verification (SMOV) plan. These data were obtained with NICMOS Camera 3 by observing at a variety of pointings. The observations are used to: 1) determine at which wavelength the HST thermal emission exceeds the zodiacal background; 2) measure the stability of the thermal emission from the telescope, by estimating dependencies of the intensity and structure of the thermal background on large slews and observation time.

2. Analysis and Discussion

The plan for the SMOV pointed thermal background test consists of taking pointed observations of blank spots of the sky with NICMOS Camera 3. Three pointings are selected: ORBIT-POLE, ANTI-SUN and a low-zodiacal-light blank spot. The first two observations were performed in consecutive orbits, to test the dependence of the telescope thermal background on large slews and observation time. In order to study the thermal background variations with respect to observation time, six sets of observations of the

ANTI-SUN were obtained only with the filter F222M. In contrast, at the third pointing the zodiacal background was observed with multiple filters to determine the wavelength at which the HST thermal emission exceeds the zodiacal light. The filters used for the last case are: F110W, F160W, F175W, F222M, and F240M.

Each observation was performed with a spiral dither pattern that included 16 exposures. For each exposure the data were taken using the MULTIACCUM readout mode. The sequence, the total exposure time per exposure and the NSAMP keyword setting are described for each target at each filter in the table below (Table 1).

Table 1. Characteristics of Observations

OBSERVATION*	FILTER	EXPOSURE TIME (sec)	NSAMP	SAMP SEQUENCE
ORBIT-POLE	F222M	63.964	10	STEP32
ANTI-SUN**	F222M	63.964	10	STEP32
LOW-BCK	F110W	191.959	12	STEP64
LOW-BCK	F160W	191.959	12	STEP64
LOW-BCK	F175W	63.964	10	STEP32
LOW-BCK	F222M	63.964	10	STEP32
LOW-BCK	F240M	31.965	9	STEP32

* 16 exposures for each observation. ** 6 sets of observations.

In this study of the data, the thermal background measurements are presented as the average count-rate calculated over the entire chip. But as mentioned in the Cycle 7-NIC-MOS Handbook, Camera 3 has a vignetting problem which affects the count-rate in rows 1 - 100 from column 1 to 256. The average count-rate is therefore computed in the area included between row 120 and row 256. This area is free from vignetting effects.

The analysis of each exposure shows a peculiar feature. In fact, figure 1 presents an example where the count-rate is systematically lower in the first 50 columns of the image. More observations are needed before reaching a conclusive understanding of the beforementioned feature.

As a consequence of this signature, the average count-rate of each exposure is estimated over three different areas each excluding the vignetting: 1) the chip area from row 120 to 256 including all columns from 1 to 256; 2) the area that shows a lower count rate (rows 120 to 256 including columns 1 to 50); and 3) the area with the slightly higher count-rate (rows 120 to 256 including columns 60 to 256). The average count-rate for these three areas, as is demonstrated in Figure 2, seems to be invariant from one exposure to another. The analysis of each of the sixteen dither pattern exposures is performed on each of the

observation sets. The results of the analysis are similar for all exposures of each pointing. Figure 2 represents an example of this analysis over one observation set. The fourth curve with the higher average count-rate is calculated over the entire chip including the vignetted area. This shows the dramatic effects of vignetting in Camera 3.

Since Figure 2, shows little variability in the thermal background from exposure to the next, the multiple exposures of the dither pattern are combined for each observation set.

The comparison of the measurements from each exposure of the ANTI-SUN observations suggests that the thermal background is stable with respect to observation time. In fact, for each data set of these observations, the multiple dither patterns are combined and an average count-rate is estimated for each observation. Figure 3 shows the results to be constant around an average count-rate of 9 ADU/sec.

As mentioned previously, all three targets (ORBIT-POLE, ANTI-SUN, ZODIACAL BACKGROUND) are observed using the F222M filter. The results of the thermal background measurements from these exposures are shown in table 2 and appear to be fairly similar for these different pointings. This reaffirms the small effect on the thermal background of large telescopes slews.

Table 2. Results from 3 Different Targets as average COUNT-RATE

TARGET	(ADU/sec)	(e/pix/sec)
ORBIT POLE	9.068	58.08
ANTI-SUN	9.004	54.02
ZODIACAL BACKGROUND	8.882	53.29

Finally, the zodiacal background is observed with five different filters. The data is processed in the same way as the ORBIT-POLE and the ANTI-SUN data. The average count-rate is computed over three different areas and the results are compared from one exposure to the next where they seem to be stable. The thermal background estimated from the low zodiacal pointing is listed for each of the five filters in table 3. The background determined with the Exposure Time Calculator seems to be quite close to the observations.

Table 3. Results from Zodiacal Background Observations as average COUNT-RATE

FILTER	OBSERVED BACKGROUND	OBSERVED BACKGROUND	ETC BACKGROUND
	(ADU/sec)	(e/pix/sec)	(e/pix/sec)
F110W	0.1288	0.77	0.71
F160W	0.1246	0.75	0.65
F175W	11.35	68.10	79.58
F222M	8.882	53.29	58.28
F240M	57.69	346.14	362.79

As part of the study of the behavior of the thermal background with time, the pointed thermal background measurement are compared to the measurements obtained during the NICMOS thermal check before and after the COSTAR arm deployment. This test was used to ascertain that the COSTAR arm does not contribute to the thermal background seen in NICMOS. The observations were performed in the beginning of SMOV months before the pointed thermal background observations. The results as shown in table 4, suggest a 10% variation in the thermal background along an extended period of time. In fact, an average count-rate is estimated from data taken before and after the deployment. The average is computed in the same method mentioned previously for filters F110W, F175W and F240W. The results of these calculations are slightly higher (by ~10%) than the ones presented in table 3.

The thermal background measured after the COSTAR arm deployment is marginally higher than that before deployment. However, the difference is small enough that it could easily be due to a change in the Sun angle of the telescope rather than being a result of COSTAR. The background count-rates observed after COSTAR deployment are very close (within a few percent) to those calculated with the NICMOS Exposure Time Calculator (ETC). They imply, when compared with the pointed thermal background observations, that the background count-rate can change by at least 10% over multiple orbit timescales. However, the data presented here do not give an indication of the length of this variation timescale. The pointed background observations suggest that so long as the pointing remains fixed the thermal background is remarkably stable on the timescales of a few orbits. The ETC appears to give a good estimate of the maximum thermal background likely to be observed, and the minimum appears to be only about 10% lower.

Table 4. Results from Observations as average COUNT-RATE (ADU/sec)

FILTER	BEFORE COSTAR	AFTER COSTAR	POINTED THERMAL BCKGRD
F110W	0.16	0.16	0.1288
F175W	11.92	12.15	11.35
F240M	61.45	62.57	57.69

As mentioned previously, one of the goals of this experiment is to determine at which wavelength the HST thermal emission exceeds the zodiacal background. Thermal background measurements were therefore obtained at various points in SMOV, including the pointed thermal background test. Based on these measurements, the approximate emissivities of the HST mirrors are determined by fitting a model of the thermal emission to the observations. This model, presented in figure 4, shows where the thermal background emission, which rises with increasing wavelength, crosses over the zodiacal background, which falls with increasing wavelength. For each camera the cross-over point is in the vicinity of 1.6-1.7 microns.

3. Conclusions and Recommendations

In this ISR we have demonstrated that the HST thermal background seems to be independent of large slews, and regardless of the pointing it is estimated to be of about 9ADU/sec (58.53 (e/pic/sec)) in the F222M filter in Camera 3. Also the observed thermal background agrees well the background determined from the exposure time calculator. However, until an analysis of a much larger set of parallel thermal background observations has been completed, we still recommend observers to obtain a background measurement at least once per orbit, as we do not yet know the timescale or causes of background changes which can be as large as 10%.

ONE ROW OF ONE EXPOSURE IMAGE

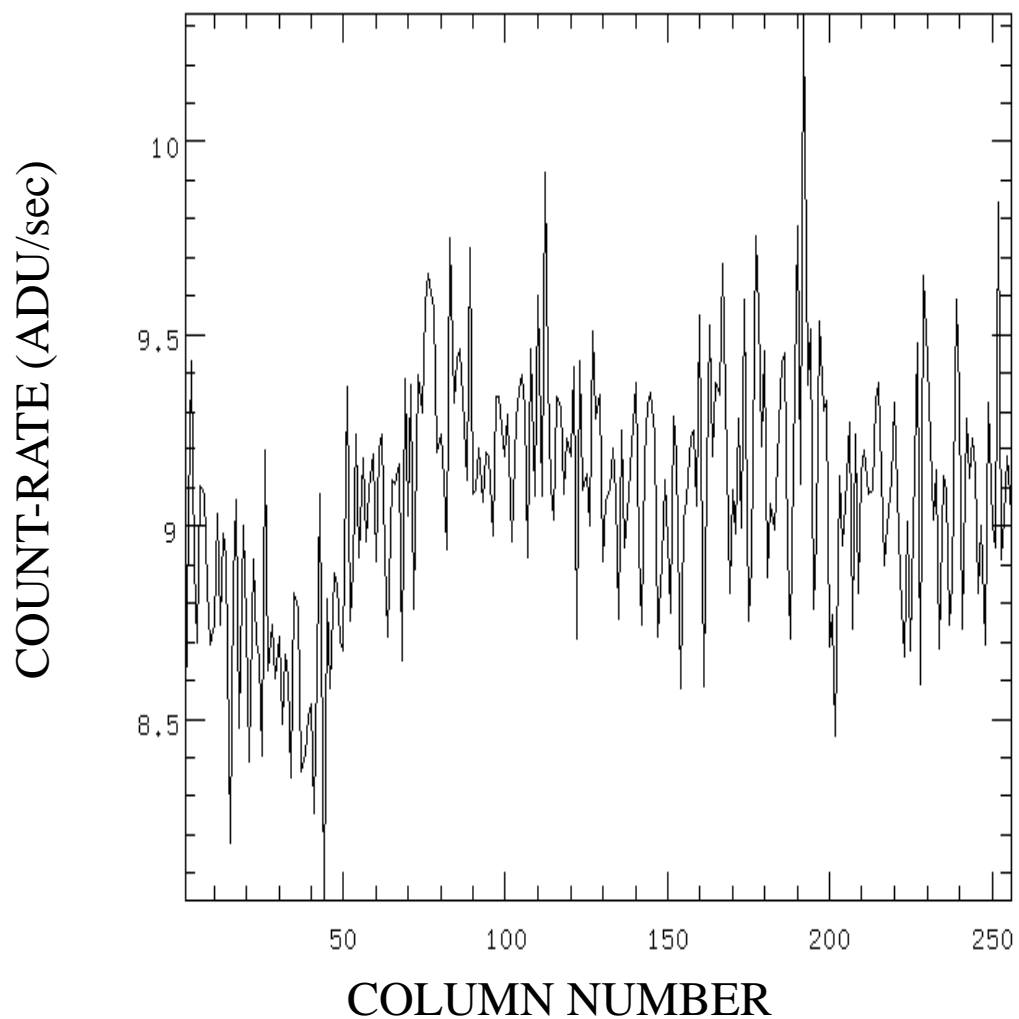


Figure 1: This figure shows an example of one exposure where the COUNT-RATE is lower in the first 50 columns of the image. This feature is present in all data sets of each of the three pointings.

16 DITHER PATTERNS OF 1 OBSERVATION

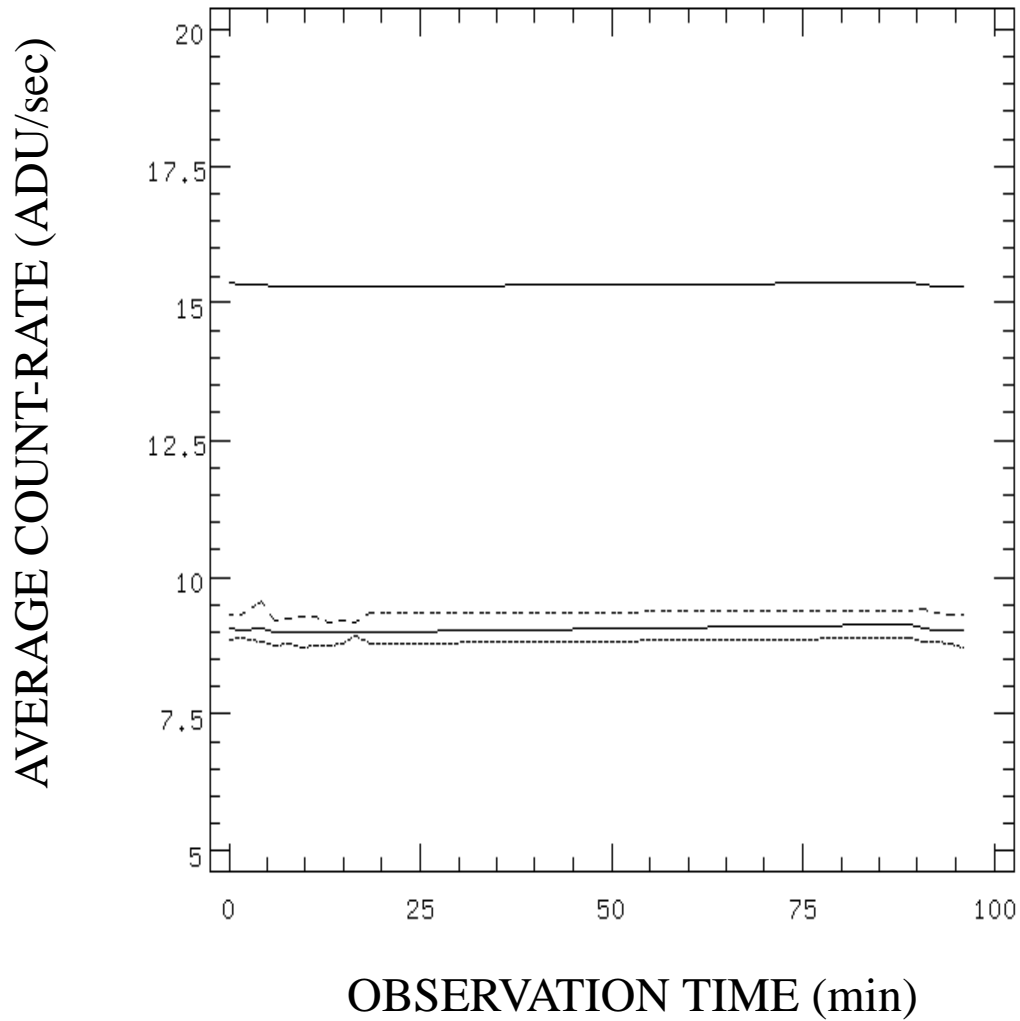


Figure 2: This figure shows an example of the results of the analysis over one observation set. (ORBIT-POLE). The average count-rate seems to be generally stable from the first dither pattern exposure to the last. This is true for all data sets of each of the three pointings. As well the average is within the same COUNT-RATE of 9 ADU/sec as shown by the first three curves (three different areas on the chip excluding the vignetted parts). The fourth curve is the average count-rate computed over the entire chip including the vignetted area. Each exposure has an exposure time of 64 seconds.

OBSERVATIONS OF THE ANTI-SUN

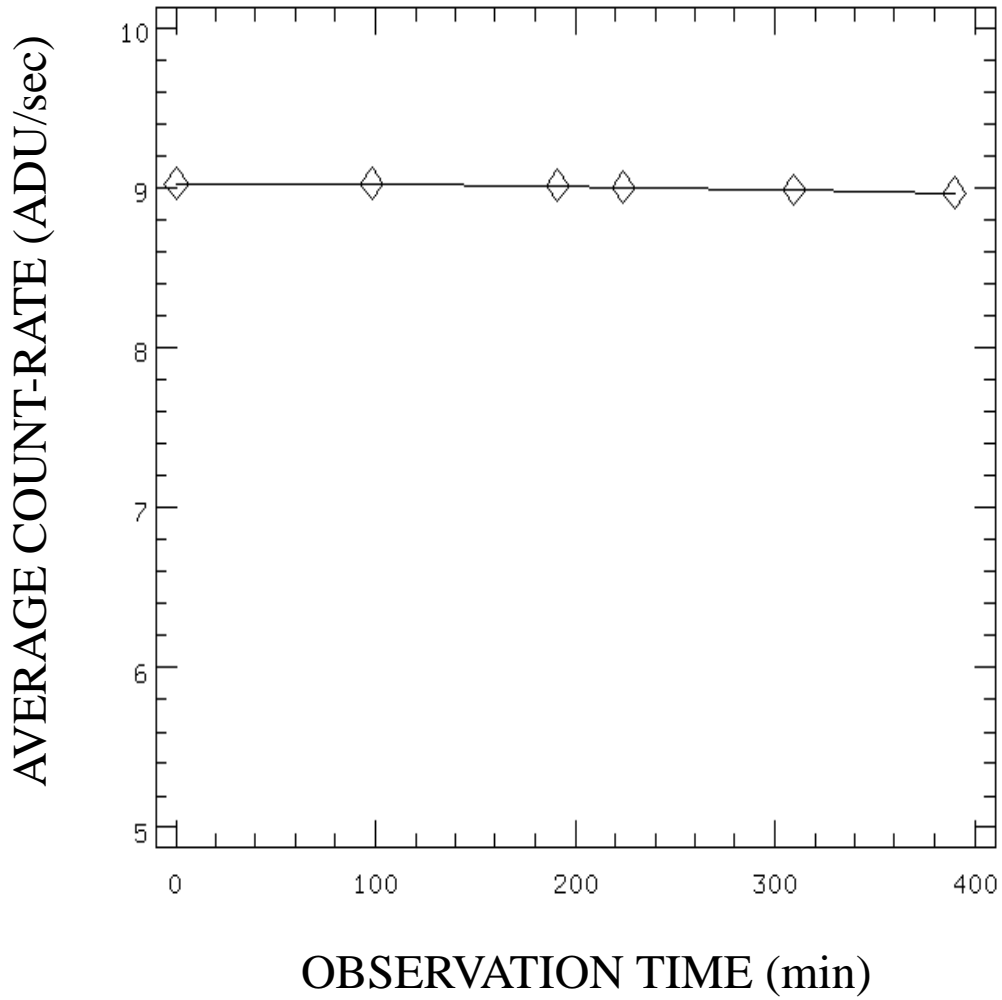


Figure 3: This figure shows the background measurements estimated with the 6 sets of ANTI-SUN observations taken consecutively with the F222M filter. Each point represents the combined average count-rate of 16 dither patterns.

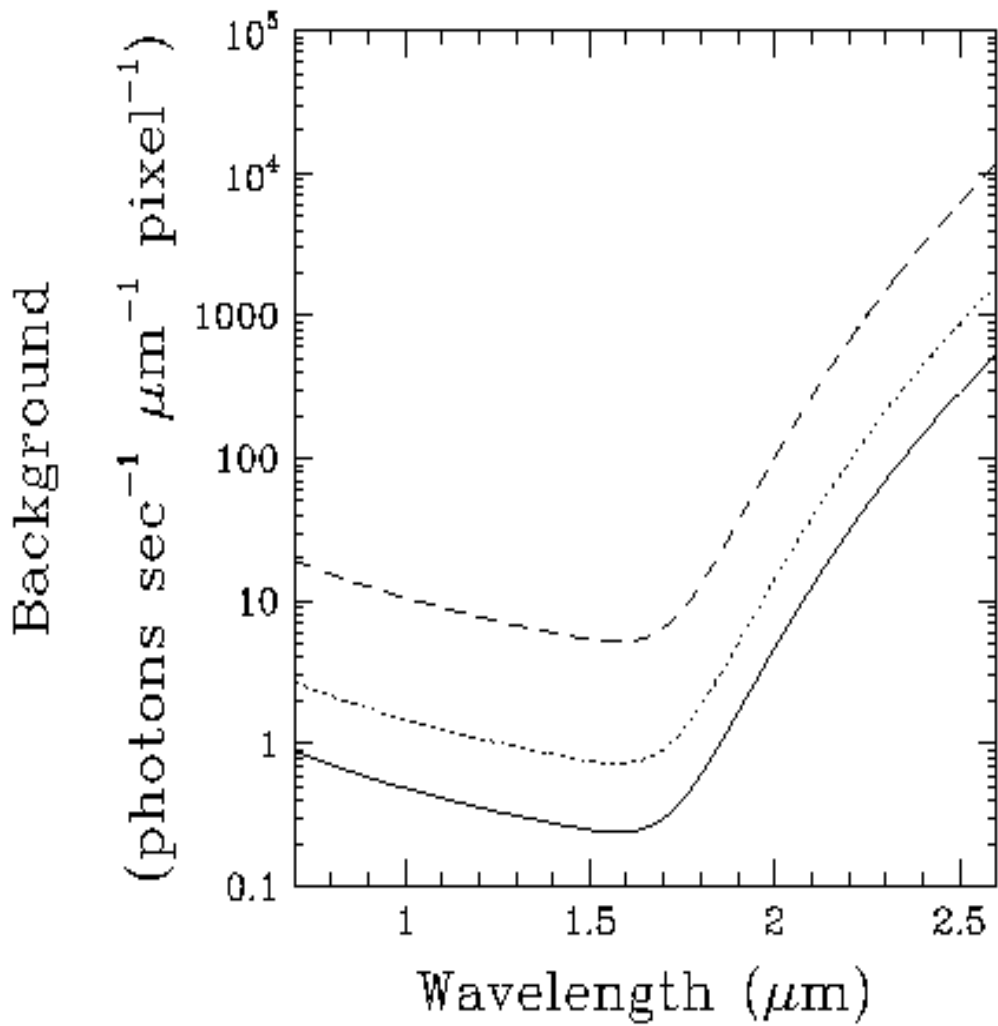


Figure 4: This figure, shows where the thermal background emission, which rises with increasing wavelength, crosses over the zodiacal background, which falls with increasing wavelength. For each camera the cross-over point is in the vicinity of 1.6-1.7 microns. The curves from bottom to top represents Cameras 1, 2 and 3.